Clinical & Experimental Metastasis **21:** 453–460, 2004.

Experimental liver metastasis: Standards for local cell implantation to study isolated tumor growth in mice

Otto Kollmar[1], Martin K. Schilling[1] & Michael D. Menger[2]
[1]*Department of General, Visceral and Vascular Surgery and* [2]*Institute for Clinical & Experimental Surgery, University of Saarland, Homburg/Saar, Germany*

Received 27 May 2004; accepted in revised form 5 August 2004

Key words: colorectal cancer, liver, metastasis, tumor, model, intravital fluorescence microscopy

Abstract

Experimental hepatic metastasis of colorectal tumors is frequently studied by local intrahepatic tumor cell implantation. However, although a variety of factors of the implantation procedure may markedly influence tumor growth characteristics, standards are not defined yet. Herein, we studied the effect of different modes of cell implantation on tumor growth and angiogenesis by *in vivo* fluorescence microscopy and histology seven days after grafting colorectal CT26.WT tumor cells into the left liver lobe of syngeneic BALB/c mice. We demonstrate that (i) radial growth of cells implanted within the central area of the lobe is inhibited by a regularly observed fissura which crosses at midline the surface of the lobe; (ii) cells suspended during implantation in RPMI show an uncontrolled overwhelming growth 40-fold of those suspended in PBS; (iii) cell implantation in 100 μl and 20 μl suspension medium is significantly more complicated by rupture of the liver capsule, uncontrolled intraparenchymal cell spread and recoil of the cells through the injection canal compared to cells suspended in 10 μl; (iv) the frequency of metastasis within the injection canal and at the puncture site is significantly reduced using 32G compared to 27G or 29G needles; (v) occlusion of the puncture site by acrylic glue or electric coagulation completely abolishes peritoneal tumor spread compared to no treatment or gentle compression by cotton gauze. We conclude that a standardized growth of isolated metastases is best achieved by implanting CT26.WT cells in a 10 μl PBS blister subcapsularly into the paramedian area of the lower surface of the left liver lobe, using a 32-gauge needle and closing the puncture site with acrylic glue.

Introduction

The liver is the most common and critical site of distant metastasis of colorectal cancer. For non-resectable hepatic metastases there is no effective therapy with curative intent available until now. Thus, experimental studies aiming at improving the understanding of the mechanisms of growth of organ-specific metastases are necessary to develop novel therapeutic strategies. During the last decade the use of mice has become of increased interest in experimental oncology, because there is a large availability of specific antibodies as well as genetically modified strains.

A variety of tumor models with properties to develop liver metastases have been introduced. The spontaneous liver metastasis model, established from a primary colon tumor, induced by colon wall injection of tumor cells, or from an artificial primary location, induced by injection of tumor cells into the spleen, represents an ideal tool to study the mechanisms of cell spread of colon cancer to the liver. The disadvantage, however, is that metastasis in this model is diffuse and variable in nature and magnitude. Thus, it may not be suitable to examine distinct characteristics of angiogenesis and growth in solitary, i.e. isolated metastatic tumors.

With the idea of mimicking the blood-borne metastatic pathway, the injection of tumor cells through the portal venous vascular system is a well-established technique to study the early steps of the complex metastatic cascade of tumor cell invasion, survival and growth [1, 2]. Nonetheless, in consequence of the overload of the biological system with unnaturally high amounts of tumor cells and due to the circulatory dynamics of tumor cell dissemination in the development of tumor metastasis, this technique has also to be considered as a diffuse liver metastasis model with some degree of variability.

The direct implantation of tumor cells into the liver parenchyma is another well-accepted model to study

Correspondence to: Kollmar Otto, MD, Department of General, Visceral and Vascular Surgery, University of Saarland, D-66421 Homburg/Saar, Germany.
Tel: +49-6841-162-2611; Fax: +49-6841-162-2697;
E-mail: chokol@uniklinik-saarland.de

growth of tumors and metastases [3–11]. This model does not allow to evaluate the individual steps of tumor cell dissemination to remote organs, and it avoids the initial contribution of various immune cells such as Kupffer cells and endothelial cells, including their potentially metastasis promoting signalling pathways [12]. In contrast to the aforementioned models, however, it ideally enables to quantitatively study angiogenesis, growth and spreading of a solitary primary hepatic tumor [13] or an isolated metastasis [14]. With the idea to examine the exact time course of tumor blood vessel formation, microcirculation and cell proliferation by *in vivo* microscopic methods [15, 16], the major advantage of this model is the potential to define the implantation site and to apply a standardized tumor cell count.

Although this model of direct intraparenchymal tumor cell implantation is frequently used in experimental cancer research, it should be taken into account that several factors of the implantation procedure may markedly influence tumor growth characteristics. Surprisingly, standards for the implantation procedure are not defined yet. Herein, we therefore studied the effect of different modes of cell implantation on tumor growth and angiogenesis after grafting colorectal CT26.WT tumor cells into the left liver lobe of syngeneic mice.

Materials and methods

Experiments were performed after approval by the local governmental ethic committee, and in accordance with the UKCCCR Guidelines for the Welfare of Animals in Experimental Neoplasia (Br J Cancer 77(1998) 1–10) and the Interdisciplinary Principles and Guidelines for the Use of Animals in Research (New York Academy of Sciences Ad Hoc Committee on Animal Research, New York).

Cell line and cell culture

The CT26 cell line is a N-nitroso-N-methylurethane-induced undifferentiated adenocarcinoma of the colon, generated in the BALB/c mouse. For our studies the cloned CT26.WT cell line (ATCC CRL-2638®, LGC Promochem GmbH, Wesel, Germany) was maintained in cell culture as monolayers in RPMI-1640 medium with 2 mM L-glutamine (Sigma-Alderich Chemie GmbH, Taufkirchen, Germany) supplemented with 10% fetal calf serum (FCS Gold, PAA Laboratories GmbH, Cölbe, Germany), 100 U/ml penicillin and 100 μg/ml streptomycin (PAA Laboratories GmbH). Cells were incubated at 37 °C in a humidified atmosphere containing 5% CO_2 in air. Only cells from the first two serial passages after cryo-storage were used for implantation.

At the day of tumor cell implantation, single cell CT26.WT suspensions were harvested from subconfluent cultures (70–85%) by 0.05% trypsin and 0.02% EDTA (PAA Laboratories GmbH). Cells were washed once in RPMI-1640 medium with FCS and twice in phosphate buffered saline solution (PBS, PAA Laboratories GmbH). An aliquot of the cell suspension was stained by trypan blue to determine cell viability and cell count. In all preparations, cell viability was $>90\%$. Cells were then pelleted by centrifugation. The sediment was resuspended in PBS solution at 1×10^5 cells/10 μl, 1×10^6 cells/20 μl or 1×10^6 cells/100 μl. In some experimental groups, CT26.WT cells were suspended for implantation in RPMI-1640 medium without FCS. The CT26.WT cells were implanted subsequently (within 5 min) after preparation. For the intravital fluorescence microscopic study of placement of tumor cells, green fluorescent protein (GFP)-transfected CT26.WT tumor cells were used.

Animals and anesthesia

Eight- to 12-week-old female BALB/c mice were purchased from Charles River Laboratories (Sulzfeld, Germany) and kept in the temperature- and humidity-controlled 12 h dark/light cycle environment of the animal care facility of the Institute for Clinical and Experimental Surgery at the University of Saarland. Animals had free access to tap water and standard pellet food.

Mice with a body weight (BW) of 18–20 g were anesthetized prior to all surgical procedures by intraperitoneal injection of 25 mg/kg BW xylacin hydrochloride (Rompun® 2%, Bayer, Leverkusen, Germany) and 125 mg/kg BW ketamine hydrochloride (Ketanest, Pharmacia GmbH, Erlangen, Germany). For intrahepatic implantation of the CT26.WT cells the anesthetized animals were placed in supine position. After laparotomy, the left liver lobe was mobilized by incision of the falciform ligament to partially free the liver from the diaphragm and to facilitate the exterioration of the left liver lobe. This allowed the direct implantation of tumor cells into the parenchyma of the lower surface of the left liver lobe.

Study parameters

Animals were allocated to different groups, which varied in the mode of tumor cell implantation. The following modes of cell implantation were analyzed: (i) implantation of tumor cells within the center area of the left liver lobe closed to the fissura crossing at midline the surface of the lobe; (ii) implantation of tumor cells within in the paramedian area of the left liver lobe; (iii) implantation of 1×10^6 tumor cells in RPMI medium; (iv) implantation of 1×10^5 tumor cells in RPMI medium; (v) implantation of 1×10^5 tumor cells in PBS solution; (vi) implantation of tumor cells in 100 μl suspension; (vii) implantation of tumor cells in 20 μl suspension; (viii) implantation of tumor cells in 10 μl suspension;

(ix) injection of only 10 μl PBS without tumor cells; (x) implantation of tumor cells with a 27G needle; (xi) implantation of tumor cells with a 29G needle; (xii) implantation of tumor cells with a 32G needle; (xiii) implantation of tumor cells with occlusion of the puncture site by acrylic glue produced from enbucrilate (Histoacryl®; B. Braun, Aesculap AG, Tuttlingen, Germany); (xiv) implantation of tumor cells with occlusion of the puncture site by electric coagulation (Bovie®, Aaron Medical, St. Petersburg, Florida); (xv) implantation of tumor cells with occlusion of the puncture site by gentle pressure for 1 min (cotton-tipped applicator stick); and (xvi) implantation of tumor cells without occlusion of the puncture site.

Tumor cells were implanted with the use of a stereo-microscope (Leica M651, Leica Microsystems AG, Heerbrugg, Switzerland). During the implantation procedure, the following parameters were documented: rupture of the liver capsule, recoil of tumor cells within the injection canal, spread of tumor cells within the liver parenchyma.

After tumor cell implantation the left liver lobe was repositioned anatomically into the peritoneal cavity, 1 ml of physiological saline was added into the abdomen to compensate for fluid loss, and the abdominal wall was then closed in a one-layer technique with a non-resorbable suture (5/0 Prolene®, Ethicon GmbH, Norderstedt, Germany).

Intravital fluorescence microscopy

Because *in vivo* microscopy represents a direct approach to monitor and quantify tumor growth and tumor blood supply on the liver surface, epi-illumination technique was performed at day seven after implantation of the tumor cells. After re-laparotomy and preparation of the liver, the animals were positioned on their left side on a plexiglas stage. The left liver lobe was gently exteriorized and placed on a mechanical stage, so that the lower surface of the liver lobe could be placed horizontal to the microscope, which guaranteed adequate focus levels for the microscopic procedure on the area of liver surface under investigation. Because under normal *in situ* conditions the left lobe of the liver is in a position that the lower surface directs almost from cranial to caudal, a relevant flexion of the feeding and draining vessels for exterioration in left-sided position was not required. To prevent drying of tissue and influence of ambient air, the lower surface of the left liver lobe was covered by a circular glass coverslip (12 mm diameter). Before *in vivo* microscopy, tumors were analyzed and documented under the Leica stereo-microscope to assess solid or diffuse growth characteristics and spread into the peritoneal cavity.

In vivo microscopy was performed using a modified Zeiss Axio-Tech microscope (Zeiss, Oberkochen, Germany) and the epi-illumination technique with a 100W mercury lamp, as previously described in detail [16]. Microscopic images were recorded by a charge-coupled device video camera (FK 6990, Prospective Measurements Inc., San Diego, California, USA) and were transferred to a video system (VO-5800 PS, Sony, Munich, Germany) for subsequent data and images analysis. With the use of a 4× long distance objective (×4/0.16, Olympus), a 10× long distance objective (×10/0.30, Zeiss) and a 20× water immersion objective (×20/0.5 w Ph2, Zeiss), magnifications of 100×, 250, and 500× were achieved on the video screen (PVM-1442 QM, diagonal: 330 mm, Sony). After contrast enhancement by intravenously applied sodium fluorescein (2 μmol/kg; Merck, Darmstadt, Germany), blue light epi-illumination (450–490/ > 520 nm excitation/emission wavelengths) allowed to assess the hepatic microvasculature, newly formed tumor blood vessels and overall tumor size. In addition, the method enabled to detect satellite tumors as well as angiogenesis and tumor growth within the injection canal and at the puncture site.

Morphological examinations

At the end of the experiment, the left liver lobe was harvested and cut into slices with a diameter of 1 mm using a Tissue Slicer (McIlwain Tissue Shopper, Saur Laborbedarf, Reutlingen, Germany). Slices in which tumor could be identified by the stereo-microscope (Leica) were documented on videotape. The size of the tumor was measured using the CapImage System (Zeintl, Heidelberg, Germany) and tumor volume was calculated by the following algorithm: tumor volume $(V) = 4/3\pi \times a/2 \times b/2 \times c/2$, where a, b, and c represent the three perpendicularly orientated diameters of the tumor. For light microscopy, formalin-fixed biopsies were embedded in paraffin. 4 μm-thick sections were cut and stained with hematoxylin and eosin according to standard procedures.

Statistical analysis

Data are expressed as means ± SEM or as percentage of the total number studied in each group. After proving the assumption of normality and homogeneity of variance across groups, differences between two groups were calculated by Student's *t*-test. Ratios were compared using χ^2 test or Fisher Exact test, respectively. Overall statistical significance was set at $P < 0.05$. Statistical analysis was performed using the software package SigmaStat (SPSS Inc., Chicago).

Results

For tumor implantation the lower surface of the left liver lobe was chosen, because this lobe can easily be exteriorized *in vivo*, and ideally allows intravital microscopic observations due to its plane surface. Intravital

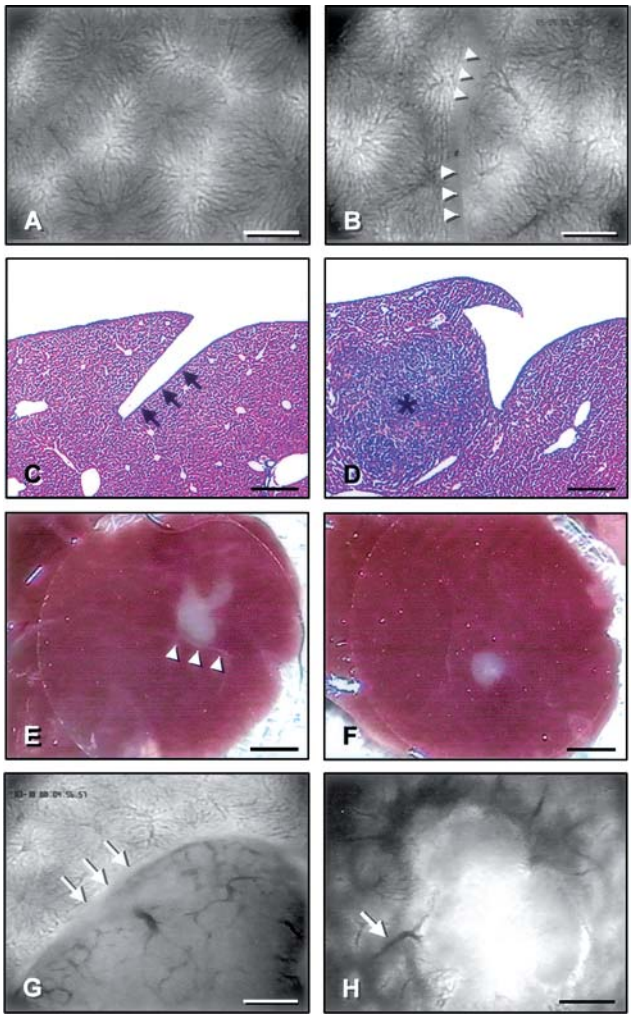

Figure 1. (A) Intravital fluorescence microscopy of the paramedian area of the lower surface of the left liver lobe. Note the homogeneous arrangement of the hepatic lobules and the sinusoidal networks within the individual hepatic lobules. (B) Intravital fluorescence microscopy of the central area of the lower surface of the left liver lobe. Note the interrupted homogeneous distribution pattern of the hepatic microvasculature due to the fissura crossing the lobe at midline (arrow heads). (C) Histomorphology confirms that the fissura at midline of the left liver lobe interrupts also the parenchymal continuity (arrows). (D) Histomorphology at day 7 after implantation of tumor cells within the central area of the left liver lobe. Note the tumor (asterisk) closely growing at the site of the fissura which crosses the lobe at midline. (E) Stereo-microscopy at day 7 after implantation of tumor cells within the central area of the left liver lobe. Note the tumor growth towards the paramedian area of the lobe, while tumor growth did not pass over the fissura crossing the lobe at midline (arrow heads). (F) Stereo-microscopy at day 7 after implantation of tumor cells within the paramedian area of the left liver lobe. Note the unaffected radial tumor growth. (G) Intravital fluorescence microscopy of the central area of the lower surface of the left liver lobe at day 7 after cell implantation. Note the lack of new blood vessel formation at the side of the tumor facing the fissura which crosses the lobe at midline (arrows). (H) Intravital fluorescence microscopy of the paramedian area of the lower surface of the left liver lobe at day 7 after cell implantation. Note the ingrowth of newly formed blood vessels (arrow) from the host tissue. Bars represent: 200 μm (A, B), 500 μm (C, D), 2000 μm (E, F), and 500 μm (G, H).

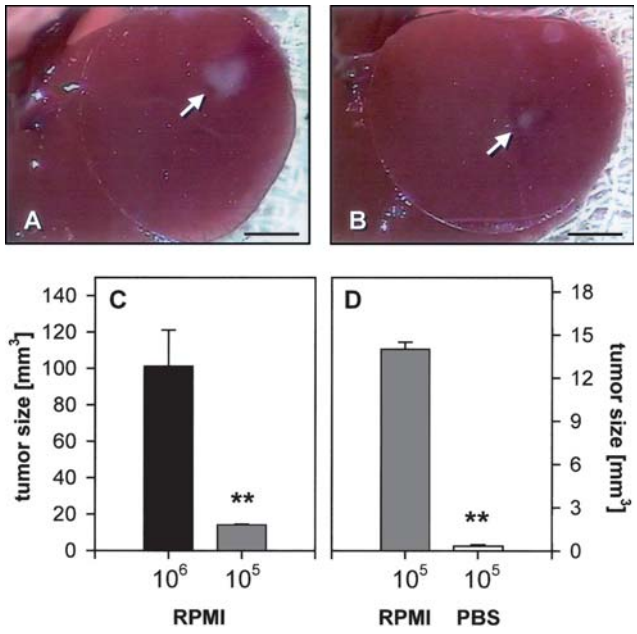

Figure 2. Stereo-microscopic imaging of tumors at day 7 after implantation of 10^5 tumor cells which were suspended in RPMI medium (A) or PBS solution (B). Note the markedly increased tumor growth if cells are injected in RPMI medium. Figure (C) displays quantitative analysis of the tumor size at day 7 after injection of 1×10^6 ($n = 8$) and 1×10^5 ($n = 8$) tumor cells in RPMI medium, while Figure (D) compares the tumor size at day 7 after injection of 1×10^5 cells in RPMI medium ($n = 8$) vs 1×10^5 cells in PBS ($n = 8$). $^{**}P < 0.01$ vs 1×10^6 RPMI medium (A) and 10^5 RPMI medium (B). Bars represent: 2500 μm (A, B).

fluorescence microscopy revealed a homogeneous arrangement of the hepatic lobules and the sinusoidal networks within the individual hepatic lobules (Figure 1A). However, in all mice the lower surface of the left liver lobe was crossed at midline by a fissura, which interrupted the homogeneous distribution pattern of the hepatic microvasculature and the liver parenchyma, as indicated by intravital microscopy (Figure 1B) and histomorphology (Figure 1C). Accordingly, tumor cells implanted within the central area of the liver lobe were affected in radial growth by the fissura in that the growing tumor did not pass over this line (Figures 1D and E). In contrast, tumor cells implanted within the paramedian area of the liver lobe were unaffected in radial tumor growth (Figure 1F). In parallel, tumor cells implanted within the central area of the lobe showed a lack of vascularization from the side facing the fissura (Figure 1G), while cells implanted in paramedian position were found vascularized in its whole circumference (Figure 1H).

The implantation of 1×10^6 tumor cells suspended in RPMI medium resulted in a massive tumor growth within 7 days, displaying a multilobular structured neoplasia with uncontrolled distribution, encompassing ~80% of the lobe. The reduction of the number of tumor cells to 1×10^5 in RPMI medium significantly reduced the size of the tumor at day 7 by a factor of 10, displaying a solid, almost round tumor mass with controlled growth dimensions (Figures 2A and C). Most interestingly, after implantation of 1×10^5 tumor cells suspended in PBS, which lacks amino acids and vitamins, the seven-day tumor volume was additionally

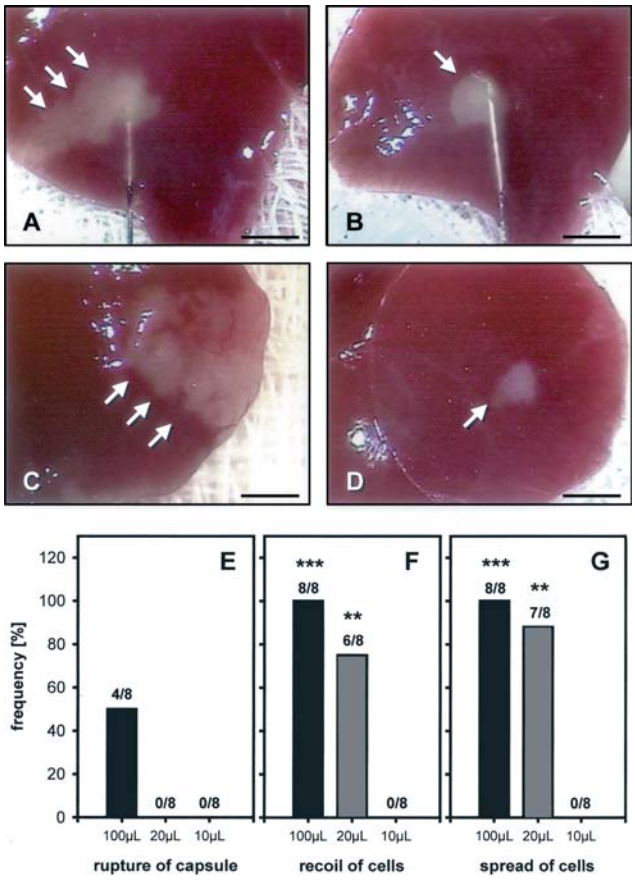

Figure 3. (A–D) Stereo-microscopy during the injection of tumor cells suspended in 20 μl (A) and 10 μl (B). Note that the large suspension volume results in uncontrolled interstitial tumor cell spread into the parenchyma (A), while the use of 10 μl suspension volume allows a standardized placement of the tumor cells within a blister beneath the liver capsule (B). Accordingly, the 20 μl suspension volume results in an inhomogeneous and uncontrolled tumor growth at day 7 after implantation (C), while cells suspended in 10μl induces a controlled growth of an isolated and rounded tumor (D). (E–G) Analysis of the frequency of rupture of the liver capsule (E), recoil of the tumor cells through the injection canal (F), and interstitial tumor cell spread into the parenchyma (G) after tumor cell implantation in suspension volumes of 100 μl, 20 μl and 10 μl, respectively. $^{**}P < 0.01$ and $^{***}P < 0.001$ vs 10 μl. Bars represent: 1600 μm (A–D).

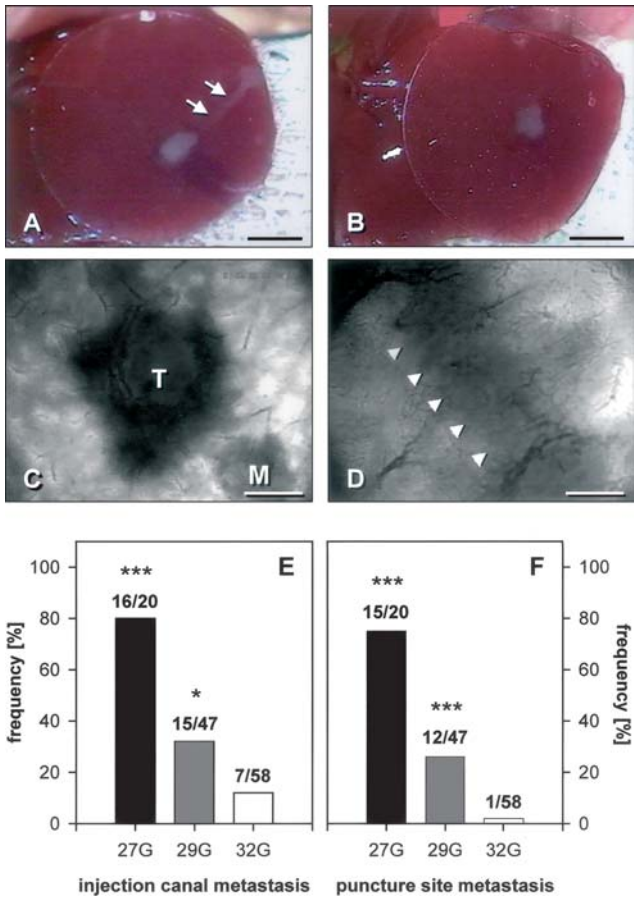

Figure 4. (A–D) Stereo-microscopy (A, B) and intravital microscopy (C, D) at day 7 after tumor cell implantation using a 27G (A, C, and D) and a 32G needle (B). Note that the use of a 27G needle is associated with tumor growth in the injection canal (A, arrows), which can impose as a vascularized, isolated satellite metastasis (C) or as a vascularized solid tumor, encompassing the entire injection canal (D, arrow heads). The use of the 32G needle for cell implantation results in a defined solid tumor growth without tumor spread within the injection canal (B). (E and F) Analysis of the frequency of injection canal metastasis (E) and puncture site metastasis (F) at day 7 after tumor cell implantation using 27G, 29G or 32G needles. $^{*}P < 0.05$; $^{***}P < 0.001$ vs 32G. T = tumor, M = satellite metastasis. Bars represent: 2500 μm (A, B) and 500 μm (C, D).

reduced by a factor of 40, indicating in these tumors a still initial state of tumor growth, which may allow to study significant mechanisms of angiogenesis and cell proliferation (Figures 2B and D).

The implantation of tumor cells in a volume of 100 μl suspension did not allow a standardized placement of the cells within the hepatic parenchyma (Figure 3). In 50% of the experiments, the implantation procedure was complicated by rupture of the liver capsule (Figure 3E), and in all cases there was a recoil of cells through the injection canal (Figure 3F) and an uncontrolled interstitial spread of the tumor cells into the parenchyma (Figures 3A and G). The interstitial spread of the cells resulted in an inhomogeneous and overwhelming tumor growth at day 7 after implantation (Figure 3C). Reduction of the cell suspension volume to 20 μl could effectively reduce the incidence of rupture of the capsule (Figure 3E), however, was not capable of preventing cell recoil and interstitial cell spread (Figures 3F and G). In contrast, the implantation of cells in a suspension volume of only 10 μl allowed to place the tumor cells ideally in a blister

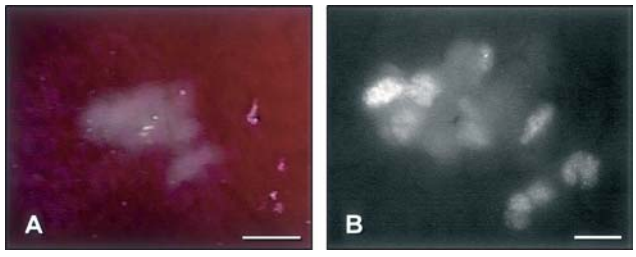

Figure 5. Stereo-microscopy (A) and intravital microscopy (B) directly after and at 20 min after implantation of GFP-transfected CT26.WT tumor cells. The intravital fluorescence microscopic technique allows exact identification of the implanted cells with high magnification. Bars represent: 1000 μm (A) and 500 μm (B).

beneath the liver capsule (Figure 3B), and was capable of completely avoiding the rupture of the capsule, the recoil of cells and the interstitial spread into the parenchyma (Figures 3E–G). This standardized placement of the tumor cells finally resulted in a controlled growth of a solitary and rounded tumor (Figure 3D). Interestingly, injection of only 10 μl PBS without tumor cells did not result in any reaction at the injection site after the 7-day period, i.e., no signs of angiogenesis, proliferation and fibrosis.

The size of the needle used for tumor cell implantation may be of particular importance. The use of a 27G needle was associated with an ~80% manifestation of puncture site and injection canal metastases (Figures 4A, E, and F). The tumor growth within the injection canal appeared as a vascularized, isolated satellite metastasis (Figure 4C) or as a vascularized solid tumor, encompassing the entire injection canal (Figures 4A and D). The use of a 29G needle for cell implantation effectively reduced the frequency of puncture site and injection canal metastasis to 32 and 26%, respectively (Figures 4E and F). Further, the use of a 32G needle almost abrogated the obstacles for standardization of the implantation procedure, displaying only 12 and 2% of injection canal and puncture site metastases (Figures 4E and F). With the use of GFP (green fluorescent protein)-transfected CT26.WT tumor cells, correct placement of the cells could also nicely be studied by intravital fluorescence microscopy (Figure 5).

Finally, the occlusion of the puncture site during cell implantation was of major importance for a standardized cell implantation procedure. If the puncture site was not occluded by any additional intervention, 100% of the experiments showed peritoneal tumor spread after the 7-day observation period (Figure 6). Gentle compression of the puncture site for 1 min with a cotton-tipped applicator stick was capable of reducing peritoneal tumor spread to 46%, while occlusion by electro-cautery or with an acrylic glue was effective to complete avoid peritoneal dissemination of the tumor cells (Figure 6).

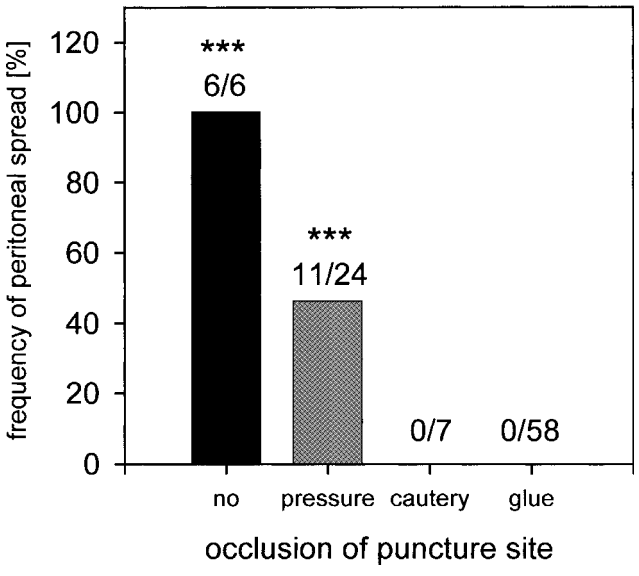

Figure 6. Analysis of the frequency of peritoneal tumor cell engraftment at day 7 after tumor cell implantation beneath the lower surface of the left liver lobe. After tumor cell injection, the puncture site was not occluded by any additional intervention (no), or was occluded for 1 min by gentle compression (pressure), by electro-cautery (cautery), or an acrylic glue (glue). ***$P < 0.001$ versus cautery and glue.

Discussion

The major finding of the present study is that the growth of an isolated hepatic tumor for experimental studies depends on the site of implantation, the number of implanted cells, the needle and the volume used for injection, and the technique applied for occlusion of the puncture site. In the murine CT26.WT tumor model, a standardized tumor growth is best achieved by injecting 1×10^5 cells in 10 μl PBS into the paramedian area of the left liver lobe using a 32G needle and closing the puncture site with acrylic glue. With the defined placement on the lower surface of the left liver lobe this experimental model is an ideal tool to study tumor growth characteristics including angiogenesis and microcirculation. The model is highly reproducible and adequately mimicks the growth characteristics of isolated hepatic tumors and metastases in the clinical setting.

The anatomy and the blood supply of the tumor hosting organ plays a pivotal role for angiogenesis and tumor growth. The lower surface of the left liver lobe is crossed at midline by a fissura, which interrupts the homogeneous distribution pattern of the hepatic microvasculature and the liver parenchyma. Although this fissura is not described in the relevant literature on the anatomy of mice, it could regularly be observed in all experiments performed. As shown by *in vivo* fluorescence microscopy, the vascular architecture at this fissura corresponds to that observed at the edges of the liver lobe, presenting with enlarged postsinusoidal venules running in parallel to each other. Our experiments show that due to the lack of new vessel formation the tumor is not capable of infiltrating into this anatomically given border during the early stage of tumor progression.

Most experimental studies with direct hepatic tumor grafting have chosen the left liver lobe for tumor cell implantation, however, no details are given on the exact placement of the cells [5, 6, 17]. From our experiments, we conclude that to achieve a standardized radial tumor growth, tumor cells should not be implanted in close vicinity of the midline fissura or the edges of the liver lobe but should rather be placed within the paramedian area of the lobés lower surface.

It is a well known phenomenon, that the incidence of artificially induced tumors depends on the tumor

cell line and correlates directly with the number of implanted cells [18]. For CT26.WT cells others have implanted cells in a range from 1×10^4 to 1×10^6, however, without indicating whether this resulted in a controlled and standardized tumor growth or whether an uncontrolled tumor spreading was observed [3, 4, 17, 19]. In our study, only with the use of 1×10^5 cells an isolated standardized grown tumor could be produced. A greater number of cells caused a significantly greater tumor mass with an overwhelming growth, encompassing almost the entire liver lobe.

Interestingly, our studies revealed that the fluid in which the cells were suspended for implantation is of pivotal relevance for tumor growth. Most authors do not provide any information on which fluid was used for cell suspension during implantation [3, 4, 6]. Of those indicating the suspension solution, most have used Hankś balanced saline solution (HBSS) [17, 19] or phosphate buffered saline solution (PBS) [7, 11, 12], while only few injected the cells suspended in medium [20]. The results of the present study show that tumor cells should be implanted in neutral suspension solutions, such as PBS, because the use of cell culture medium masks the normal characteristics of tumor growth by initiating excessive tumor masses already seven days after implantation.

Because the liver of mice is enveloped by an only thin capsule, the implantation of tumor cells beneath the capsule has to be considered intrahepatically. To generate an isolated tumor, it is necessary to avoid interstitial spreading of the tumor cells during implantation, which can be achieved by creating a blister within the subcapsular space. This may substantially depend on the volume of the tumor cell suspension injected. Most of the previous studies with direct tumor implantation in mouse liver do not indicate the cell suspension volume used [4, 5, 9], while others have reported volumes from 10 μl [8, 17, 19] and 20 μl [7, 21] to up to 100 μl of suspension [6, 10, 12]. Our experiments demonstrate that the application of a suspension volume of 100 μl is frequently associated with a rupture of the liver capsule, while application of 20 μl induces spreading of tumor cells during implantation, resulting in diffuse infiltrative and uncontrolled tumor growth during the further time course. Importantly, the interstitial spreading of cells could be effectively prevented by minimizing the volume of the cell suspension to 10 μl. This volume proved ideal to create localized and standardized blisters for tumor cell implantation.

Furthermore, the needle used for injection of the tumor cells may determine the quality of tumor cell implantation. Most reports do not give information on the needle used [4, 5, 7, 9]. Others indicate that tumor cell injection was performed with 25G [22], 26G [11, 21], 27G [10, 20] or 30G needles [6, 8, 17, 19]. The present study shows that injection of the tumor cells by a 27G needle is associated with an ~80% rate of injection canal and puncture site metastases. This frequency could be reduced by using a 29G needle, and could be almost completely abrogated by using a 32G needle. Importantly, we used 25 μl Hamilton syringes for injection, because in our experience syringes containing a volume of more than 25 μl do not allow a fine coordinated application of the 10 μl suspension.

Finally, immediately after withdrawal of the injection needle, different techniques have been suggested to prevent recoil of the injected tumor cells through the injection canal but also to prevent bleeding. While most authors do not indicate any preventive measures [4–6], others intended to occlude the injection canal at the puncture site by gentle compression with cotton gauze for 1 min [17, 19, 22], electro-cautery [8], or acrylic glue [23]. Our experiments demonstrate 100% peritoneal tumor spread after the 7-day observation period if no occlusion after cell implantation was performed. Gentle compression of the puncture site reduced peritoneal tumor spread to ~50%, while occlusion by electro-cautery and acrylic glue was effective to completely avoid peritoneal tumor cell dissemination. Of interest, the use of acrylic glue may be preferred, because the thermal tissue injury induced by electro-cautery results in massive adhesions at day 7 after implantation, which made *in vivo* microscopic analysis of those tumors extremely difficult. Within this context, it may also be mentioned that it is important to puncture the liver capsule at the edge of the liver lobe far distant from the area of final tumor cell placement. This reduces adhesions during the later time course within the area of the tumor, and avoids recoil of cells due to the extended length of the injection canal. Because *in vivo* fluorescence microscopy represents a highly sensitive method to study angiogenesis, microcirculation and tumor growth [24–26], it should additionally be taken into account that the liver tissue has to be handled carefully, avoiding to touch the lower surface of the left lobe where the tumor is implanted. Thus, all procedures may be performed with the use of stereo-microscopy and microsurgical instruments.

The value of experimental tumor models in relation to human conditions may be critically discussed. The CT26 tumor cell line, however, is a widely used, well accepted model of colon carcinoma [3–11], showing tumor growth and metastasis in mice comparable to that of human tumors. A variety of studies have reported in CT26 tumors on mechanisms of tumor-stromal interactions [27], cell-extracellular matrix adhesion [28] and fibronectin – α4, α5, αv and β1-integrin attachment [29]. Additional studies have analyzed the immune response, including lymphocyte infiltration and CD8+ action, and potential approaches for anti-tumor immune therapy [4–6, 8, 9, 30–32]. Thus, we feel that the tumor cell line studied herein is adequate to represent a model closely related to conditions known from human colorectal cancer.

In conclusion, we demonstrate that a variety of factors of the implantation procedure affect the characteristics of tumor growth and expansion. Our results indicate that a standardized growth of a solitary tumor in the mouse liver can only be achieved when tumor cells are implanted in low volume neutral solutions into the paramedian area of the lower surface of the left liver lobe using a 32-gauge needle and closing the puncture site with acrylic glue.

Acknowledgements

We appreciate the excellent technical assistance of Christina Marx and Janine Becker. This study was supported by a grant of the Medical Faculty of the University of Saarland (HOMFOR-A/2003/1).

References

1. Chambers AF, Groom AC, MacDonald IC. Dissemination and growth of cancer cells in metastatic sites. Nat Rev Cancer 2002; 2(8): 563–72.
2. Chambers AF, MacDonald IC, Schmidt EE et al. Clinical targets for anti-metastasis therapy. Adv Cancer Res 2000; 79: 91–121.
3. Topf N, Worgall S, Hackett NR, Crystal RG. Regional 'prodrug' gene therapy: Intravenous administration of an adenoviral vector expressing the *E. coli* cytosine deaminase gene and systemic administration of 5-fluorocytosine suppresses growth of hepatic metastasis of colon carcinoma. Gene Ther 1998; 5(4): 507–13.
4. Weber SM, Shi F, Heise C et al. Interleukin-12 gene transfer results in CD8-dependent regression of murine CT26 liver tumors. Ann Surg Oncol 1999; 6(2): 186–94.
5. Chen SH, Pham-Nguyen KB, Martinet O et al. Rejection of disseminated metastases of colon carcinoma by synergism of IL-12 gene therapy and 4-1BB costimulation. Mol Ther 2000; 2(1): 39–46.
6. Hirschowitz EA, Naama HA, Evoy D et al. Regional treatment of hepatic micrometastasis by adenovirus vector-mediated delivery of interleukin-2 and interleukin-12 cDNAs to the hepatic parenchyma. Cancer Gene Ther 1999; 6(6): 491–8.
7. Nakanishi K, Sakamoto M, Yasuda J et al. Critical involvement of the phosphatidylinositol 3-kinase/Akt pathway in anchorage-independent growth and hematogeneous intrahepatic metastasis of liver cancer. Cancer Res 2002; 62(10): 2971–5.
8. Huang H, Chen SH, Kosai K et al. Gene therapy for hepatocellular carcinoma: Long-term remission of primary and metastatic tumors in mice by interleukin-2 gene therapy *in vivo*. Gene Ther 1996; 3(11): 980–7.
9. Caruso M, Pham-Nguyen K, Kwong YL et al. Adenovirus-mediated interleukin-12 gene therapy for metastatic colon carcinoma. Proc Natl Acad Sci USA 1996; 93(21): 11302–6.
10. Kuo TH, Kubota T, Watanabe M et al. Liver colonization competence governs colon cancer metastasis. Proc Natl Acad Sci USA 1995; 92(26): 12085–9.
11. Kuriyama S, Yamazaki M, Mitoro A et al. Hepatocellular carcinoma in an orthotopic mouse model metastasizes intrahepatically in cirrhotic but not in normal liver. Int J Cancer 1999; 80(3): 471–6.
12. Kan Z, Ivancev K, Lunderquist A et al. *In vivo* microscopy of hepatic metastases: Dynamic observation of tumor cell invasion and interaction with Kupffer cells. Hepatology 1995; 21(2): 487–94.
13. Takamura M, Sakamoto M, Genda T et al. Inhibition of intrahepatic metastasis of human hepatocellular carcinoma by Rho-associated protein kinase inhibitor Y-27632. Hepatology 2001; 33(3): 577–81.
14. Broitman SA, Wilkinson J IV, Cerda S, Branch SK. Effects of monoterpenes and mevinolin on murine colon tumor CT-26 in vitro and its hepatic "metastases" *in vivo*. Adv Exp Med Biol 1996; 401: 111–30.
15. Menger MD, Laschke MW, Amon M et al. Experimental models to study microcirculatory dysfunction in muscle ischemia-reperfusion and osteomyocutaneous flap transfer. Langenbecks Arch Surg 2003; 388(5): 281–90.
16. Menger MD, Marzi I, Messmer K. *In vivo* fluorescence microscopy for quantitative analysis of the hepatic microcirculation in hamsters and rats. Eur Surg Res 1991; 23(3–4): 158–69.
17. Suh KW, Piantadosi S, Yazdi HA et al. Treatment of liver metastases from colon carcinoma with autologous tumor vaccine expressing granulocyte-macrophage colony-stimulating factor. J Surg Oncol 1999; 72(4): 218–24.
18. Fisher ER, Fisher B. Experimental studies of factors influencing hepatic metastases. I. The effect of number of tumor cells injected and time of growth. Cancer 1959; 12(5): 926–28.
19. Hanes J, Sills A, Zhao Z et al. Controlled local delivery of interleukin-2 by biodegradable polymers protects animals from experimental brain tumors and liver tumors. Pharm Res 2001; 18(7): 899–906.
20. Chan WS, Page CM, Maclellan JR, Turner GA. The growth and metastasis of four commonly used tumour lines implanted into eight different sites: Evidence for site and tumour effects. Clin Exp Metast 1988; 6(3): 233–44.
21. Genda T, Sakamoto M, Ichida T et al. Cell motility mediated by rho and Rho-associated protein kinase plays a critical role in intrahepatic metastasis of human hepatocellular carcinoma. Hepatology 1999; 30(4): 1027–36.
22. Chen MC, Tsang YM, Stark DD et al. Hepatic metastases: Rat models for imaging research. Magn Reson Imaging 1989; 7(1): 1–8.
23. Isbert C, Boerner A, Ritz JP et al. *In situ* ablation of experimental liver metastases delays and reduces residual intrahepatic tumour growth and peritoneal tumour spread compared with hepatic resection. Br J Surg 2002; 89(10): 1252–9.
24. Schäfer T, Scheuer C, Roemer K et al. Inhibition of p53 protects liver tissue against endotoxin-induced apoptotic and necrotic cell death. FASEB J 2003; 17(6): 660–7.
25. Schüder G, Vollmar B, Richter S et al. Epi-illumination fluorescent light microscopy for the *in vivo* study of rat hepatic microvascular response to cryothermia. Hepatology 1999; 29(3): 801–8.
26. Vajkoczy P, Farhadi M, Gaumann A et al. Microtumor growth initiates angiogenic sprouting with simultaneous expression of VEGF, VEGF receptor-2, and angiopoietin-2. J Clin Invest 2002; 109(6): 777–85.
27. Kubota T, Fujiwara H, Amaike H et al. Reduced HGF expression in subcutaneous CT26 tumor genetically modified to secrete NK4 and its possible relation with antitumor effects. Cancer Sci 2004; 95: 321–7.
28. Lee JH, Seo YW, Park SR et al. Expression of a splice variant of KAI1, a tumor metastasis suppressor gene, influences tumor invasion and progression. Cancer Res 2003; 63: 7247–55.
29. Geng L, Ali SA, Marshall JF et al. Fibronectin is chemotactic for CT 26 colon carcinoma cells: Sub-lines selected for increased chemotaxis to fibronectin display decreased tumorigenicity and lung colonization. Clin Exp Metast 1998; 16: 683–91.
30. Rabau M, Kashtan H, Baron S et al. Inhibition of CT-26 murine adenocarcinoma growth in the rectum of mice treated with recombinant human interleukin-6. J Immunother Emphasis Tumor Immunol 1994; 15: 257–64.
31. Saffran DC, Horton HM, Yankauckas MA et al. Immunotherapy of established tumors in mice by intratumoral injection of interleukin-2 plasmid DNA: Induction of CD8+ T-cell immunity. Cancer Gene Ther 1998; 5: 321–30.
32. Ali S, Ahmad M, Lynam J et al. Trafficking of tumor peptide-specific cytotoxic T lymphocytes into the tumor microcirculation. Int J Cancer 2004; 110: 239–44.